

Improved Pre-charging Method for MMC-Based HVDC Systems Operated in Nearest Level Control

Kyo-Min Kim*, Jae-Hyuk Kim*, Do-Hyun Kim*, Byung-Moon Han†, and Jun-Young Lee*

*†Department of Electrical Engineering, Myongji University, Yongin, Korea

Abstract

Recently the researches on modular multi-level converter (MMC) are being highlighted because high quality and efficient power transmission have become key issues in high voltage direct current (HVDC) systems. This paper proposes an improved pre-charging method for the sub-module (SM) capacitor of MMC-based HVDC systems, which operates in the nearest level control (NLC) modulation and does not need additional circuits or pulse width modulation (PWM) techniques. The feasibility of the proposed method was verified through computer simulations for a scaled 3-phase 10kVA MMC with 12 SMs per each arm. Hardware experiments with a scaled prototype have also been performed in the lab to confirm the simulation results.

Key words: High voltage direct current (HVDC) systems, Modular multilevel converter (MMC), Nearest level control (NLC), Pre-charging method, Sub-module (SM) capacitors

I. INTRODUCTION

The modular multilevel converter (MMC) has been recognized as the most competitive converter in high voltage direct current (HVDC) systems. A number of studies on the MMC have been actively conducted for HVDC system applications [1]-[6]. Since the MMC is composed of many sub-modules (SMs) connected in series, the operation voltage and power rating can be easily raised by adding the number of SMs. In addition, the system reliability can be improved by utilizing redundant SMs [7],[8].

Due to these advantages, a lot of attention has been paid to the MMC and a number of studies on the modeling, modulation techniques, circulation current reduction, voltage balancing techniques, and control techniques for SMs failures have been conducted for improving performance [9]-[13].

The start-up process of the MMC has not drawn a lot of attention compared with its normal or abnormal operation. However, the start-up process of the MMC is more complicated than that of two-level or multi-level converters because the MMC has a lot of SM capacitors isolated each other.

In MMC-based HVDC systems, two MMCs are connected

in the back-to-back manner. When the rectifier-side MMC is connected to a 3-phase AC source, the SM capacitors are slowly charged up to the line-to-line voltage divided by the number of SMs per arm. The SM capacitor voltage rises slowly to its nominal value after operating the voltage control for a certain amount of time. However, in the inverter-side MMC, the SM capacitors are slowly charged up to the $V_{dc}/2N$, which is the DC link voltage divided by the number of SMs per leg. Therefore, a charging process from $V_{dc}/2N$ to V_{dc}/N with a relatively low transient current is required, which is called a pre-charging process. Without a pre-charging process, a large transient current flows into the SM capacitors and causes current stresses to the switching devices or filters [14].

In the early period of research, most studies have been concentrated on using additional circuits to charge the SM capacitors. One of the simplest charging circuits consists of resistances connected in series with voltage sources, in which each SM capacitor is sequentially charged. However, an additional cost is required and charging takes rather longer time due to the sequential operation [15].

To reduce the drawbacks of this method, a simultaneous charging method has been proposed by adding four thyristors per each SM. This method charges the SM capacitors through simultaneously connecting the voltage sources to all of the SM capacitors. However, it still has a big disadvantage due to adding complicated circuits [16].

A pre-charging method utilizing RLC resonance has been

Manuscript received Aug. 29, 2016; accepted Nov. 11, 2016
Recommended for publication by Associate Editor Liqiang Yuan.

†Corresponding Author: erichan@mju.ac.kr

Tel: +82-330-6366, Fax: +82-330-6814, Myongji University

*Department of Electrical Engineering, Myongji University, Korea

proposed to improve the charging speed by inserting a separate circuit into the upper and lower arms, which consists of a resistance and a switch connected in parallel. Once the charging is completed, the resistances are bypassed through parallel-connected switches under normal operation. However, additional cost is a big issue due to large rating switches and resistances [17].

A pre-charging method using PWM switching techniques without additional circuits was proposed. This method generates PWM switching pulses after comparing a certain gradient reference with the carriers, and then applies these PWM pulses for the SM. Here, the duty ratio is gradually decreased from 1 to 0, thereby bypassing two SMs inserted into each leg from $2N$ to N . This method has to be implemented with a voltage balancing algorithm and the inserted SMs are determined accordingly. So, its control is rather complicated [18].

In [19], a feed-forward control for SM capacitors was proposed for pre-charging when the MMC operates in a phase-shift carrier PWM. The average voltage control has a double loop structure in which a circulating current control is included in the inner loop. The feed-forward control offers a fast response in pre-charging, and the reference voltage increases with a constant slope. However, this scheme requires complicated design procedures.

When MMC-based HVDC systems is operated in NLC modulation, the pre-charging scheme was not dealt in the previous researches. This paper proposes a new pre-charging method for SM capacitors in MMC-based HVDC systems operated with the NLC modulation. The proposed method generates a reference signals that consists of the sum of a cosine function with a constant frequency and a ramp function with a constant gradient. Computer simulations were conducted to verify the proposed method. Experiments with a scaled prototype were conducted to verify the proposed method from a hardware point of view.

II. MMC OPERATED IN NLC MODULATION

A. MMC Power Circuit

Fig. 1 shows a power circuit of a 3-phase MMC in which N number of SMs are connected in series at the upper and lower arms of each phase leg. Each SM consists of two IGBT switches and one DC capacitor. Each SM forms the output voltage with the capacitor voltage or zero voltage, according to the switching state of two IGBT switches. The DC capacitor in the SM is charged or discharged according to the arm current direction by the switching control of two IGBTs. Each arm has an arm reactor to mitigate the circulating current at the phase legs. The output terminal of each phase has an AC filter to reduce the harmonics of the output current.

B. MMC Operation Analysis

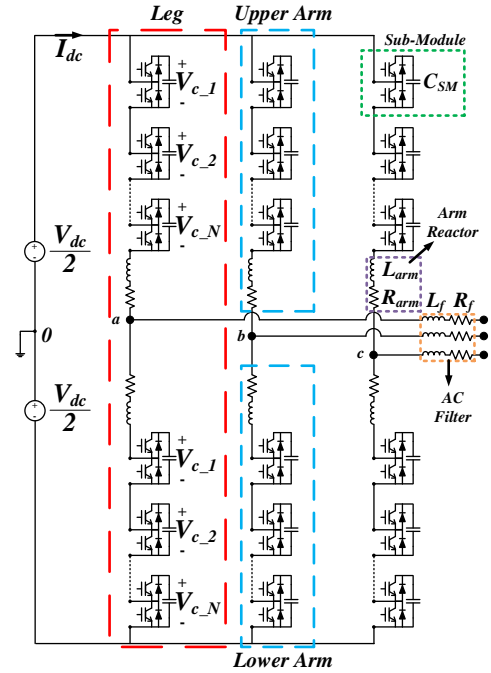


Fig. 1. Power circuit of 3-phase MMC with N SMs

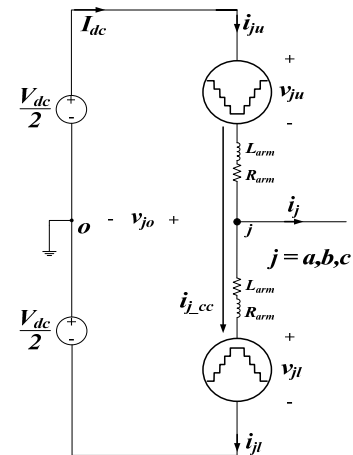


Fig. 2. Single-phase equivalent circuit of MMC.

Fig. 2 shows an equivalent circuit of a single-phase MMC with regard to the legs of the j -phase ($j = a, b, c$). In the circuit, v_{jo} refers to the output terminal voltage, and v_{ju} and v_{jl} refer to the output voltage formed at the upper and lower arms of the j -phase. i_{ju} and i_{jl} refer to the currents flowing in the upper and lower arms, $i_{j,cc}$ refers to the circulating current flowing in the j -phase leg, and i_j refers to the j -phase line current [9],[11].

Voltage Eqs. (1)-(2) can be induced through Kirchhoff's voltage law (KVL) as shown in Fig. 3. Current Equ. (3) can be induced through Kirchhoff's current law (KCL).

$$v_{jo} = \frac{V_{dc}}{2} - v_{ju} - R_{arm} i_{ju} - L_{arm} \frac{di_{ju}}{dt} \quad (1)$$

$$v_{jo} = -\frac{V_{dc}}{2} + v_{jl} + R_{arm} i_{jl} + L_{arm} \frac{di_{jl}}{dt} \quad (2)$$

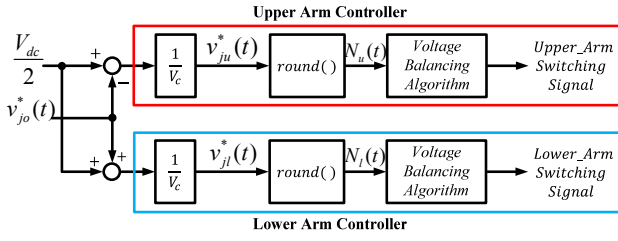


Fig. 3. Control diagram of NLC modulation method.

$$i_j = i_{ju} - i_{jl} \quad (3)$$

v_{jo} can be rearranged to Equ. (4) by solving the simultaneous equations of Eqs. (1)-(3).

$$v_{jo} = e_j - \frac{1}{2} \left(R_{arm} + L_{arm} \frac{d}{dt} \right) i_j \quad (4)$$

e_j is determined through the voltage in the upper and lower arms and can be expressed as shown in Equ. (5). Here, the phase of v_{jo} is the same phase as that of v_{jl} and there is a 180° difference with that of v_{ju} .

$$e_j = -\frac{v_{ju} - v_{jl}}{2} \quad (5)$$

C. NLC Modulation

Fig. 3 shows a control block diagram of the general NLC modulation. The controller consists of upper and lower arm controllers. The output voltage reference $v_{jo}^*(t)$ is shown in Equ. (6) and the modulation index MI is shown in Equ. (7) [20].

$$v_{jo}^*(t) = \frac{V_{dc}}{2} MI \cos(2\pi ft) \quad (6)$$

$$MI = \frac{|v_{jo}|}{V_{dc}/2}, (0 \leq MI \leq 1) \quad (7)$$

The voltage V_c in the SM capacitors at normal condition is expressed as shown in Equ. (8) and N refers to the number of SMs per each arm.

$$V_c = \frac{V_{dc}}{N} \quad (8)$$

The reference voltages for the upper and lower arms $v_{ju}^*(t)$ and $v_{jl}^*(t)$ are the control references to calculate the number of inserted SMs, in which $v_{jo}^*(t)$ can be calculated by a scale adjustment as shown in Eqs. (9)-(10).

$$v_{ju}^*(t) = \frac{1}{V_c} \left(\frac{V_{dc}}{2} - v_{jo}^*(t) \right) \quad (9)$$

$$v_{jl}^*(t) = \frac{1}{V_c} \left(\frac{V_{dc}}{2} + v_{jo}^*(t) \right) \quad (10)$$

The number of inserted SMs in the upper arm $N_u(t)$ and lower arm $N_l(t)$ can be calculated by applying a round function for $v_{ju}^*(t)$ and $v_{jl}^*(t)$ as shown in Eqs. (11)-(12).

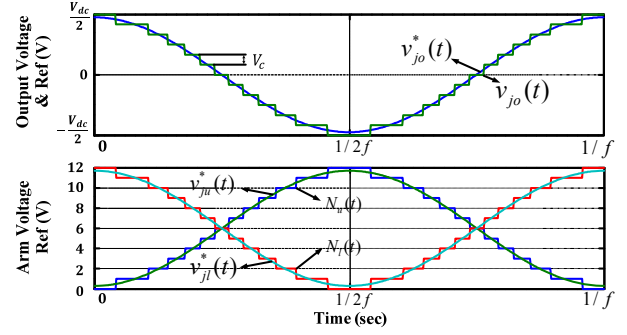


Fig. 4. Operating waveforms in NLC modulation.

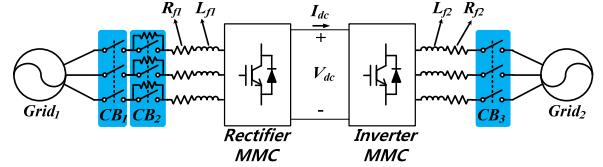


Fig. 5. MMC Back-to-Back Configuration.

A round function returns a rounded value of the input number. For example, an output of $round(2.5)$ is 3. $N_u(t)$ and $N_l(t)$ operate SMs at the upper and lower arms after generating switching pulses at the SMs through the voltage balancing algorithm.

$$N_u(t) = round(v_{ju}^*(t)) \quad (11)$$

$$N_l(t) = round(v_{jl}^*(t)) \quad (12)$$

Fig. 4 shows the operating waveforms of the NLC modulation when N is 12, MI is 0.5, V_{dc} is 1000V, and f is 60Hz. The values of MI , V_{dc} , and f are plugged into Equ. (6) to calculate $v_{jo}^*(t)$, which is $475\cos(120\pi t)$. Here, $v_{ju}^*(t)$ and $v_{jl}^*(t)$ are located in the range of 0 to 12. The sum of $N_u(t)$ and $N_l(t)$ after rounding the above calculated number is always equal to N . $N_u(t)$ and $N_l(t)$ as well as the voltage balancing algorithm determine the number of inserted SMs in the upper and lower arms thereby producing step-shape output voltage $v_{jo}(t)$ in which the step-size is V_c .

III. PRE-CHARGING MMC-BASED HVDC SYSTEM

A. MMC-based BTB HVDC Start-up Procedure

Fig. 5 shows a configuration of MMC-based back-to-back (BTB) HVDC system, in which two 3-phase MMCs with N numbers of SM per arm are connected together with common DC voltage. It is assumed that the active power flows from the grid₁ to grid₂. The rectifier MMC is coupled with the AC grid through two circuit breakers CB_1 and CB_2 for separating the DC system from the AC system, and reducing the charging speed through a resistor connected in parallel. The inverter MMC is coupled with the AC grid through a circuit breaker CB_3 . There are three stages for starting up the MMC-based HVDC system which are described in the

following.

Stage 1 (CB_1 On, CB_2 Off, CB_3 Off): The AC current from the Grid₁ flows through the pre-charging resistor and charges the SM capacitors of the rectifier MMC. Since no switching signal applies to the gate of IGBTs in SMs, the charging current flows through the diodes in SMs and the DC voltage V_{dc} slowly builds up to the line-to-line voltage $\sqrt{2}V_{LL}$, which charges the SM capacitors in the inverter MMC upto $\sqrt{2}V_{LL}/2N$.

Stage 2 (CB_1 On, CB_2 On, CB_3 Off): The SM capacitor voltage is raised up to the nominal value V_{dc}/N by applying the gate signals to the SMs and operating in voltage control. In case of the inverter MMC, since the gating signal was not applied, the SM capacitors in each leg are charged up to $V_{dc}/2N$.

Stage 3 (CB_1 On, CB_2 On, CB_3 On): After connecting the inverter MMC to the Grid₂, the SM capacitor voltage is raised upto the nominal value V_{dc}/N by applying the gate signals to the SMs and operating the current control to reduce the transient charging current.

B. Charging Process for SM capacitors in MMCs

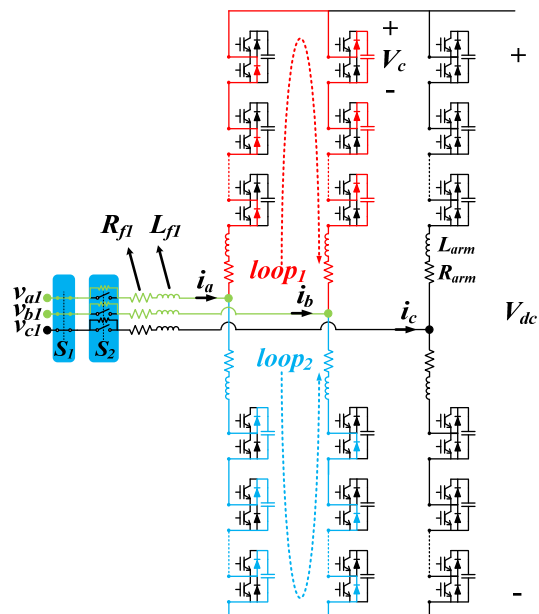
In Fig. 6(a), suppose that the MMC is connected to phases A and B, and that the current paths are formed like Loop 1 and 2. Since the current i_a is positive and the current i_b is negative, the SM capacitors of the upper arm in Phase A and those of the lower arm in Phase B are not charged, while the SM capacitors of the upper arm in Phase B and those of the lower arm in Phase A are charged upto $\sqrt{2}V_{LL}/N$. Through this process, all of the SM capacitors in the rectifier MMC are charged upto $\sqrt{2}V_{LL}/N$.

In Fig. 6(b), it is assumed that the SM capacitors in the rectifier MMC are charged up to the nominal voltage V_{dc}/N and the DC link voltage is V_{dc} . When V_{dc} is applied to the DC link of the inverter MMC, the $2N$ number of SM capacitors in each leg are charged up to $V_{dc}/2N$ through the current path shown in the figure.

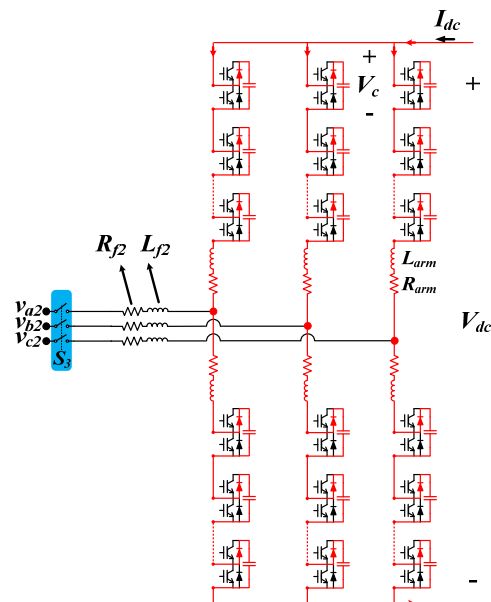
In order to increase the SM capacitor voltage up to V_{dc}/N , the inverter MMC starts to operate in current control to charge the SM capacitors without a high transient current which brings about damage on the switching devices and filters. Therefore, a pre-charging method is required in the initial startup process for MMC-based BTB HVDC systems.

IV. PROPOSED PRE-CHARGING METHOD

Fig. 7 shows a control diagram of the proposed pre-charging method. $v_{pc}^*(t)$ refers to the pre-charging reference expressed in Equ. (13), which is the sum of the N number of SMs, the ramp function $v_{ramp}^*(t)$ with a gradient constant α over time, and a cosine function $v_{cos}^*(t)$ with amplitude β and frequency f .



(a) Rectifier MMC.



(b) Inverter MMC.

Fig. 6. Charging current path in MMCs before applying gate signals.

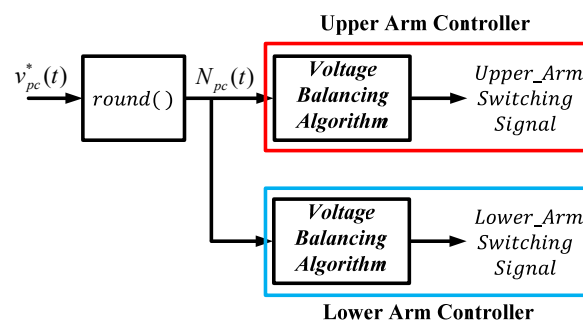


Fig. 7. Control diagram of proposed pre-charging method.

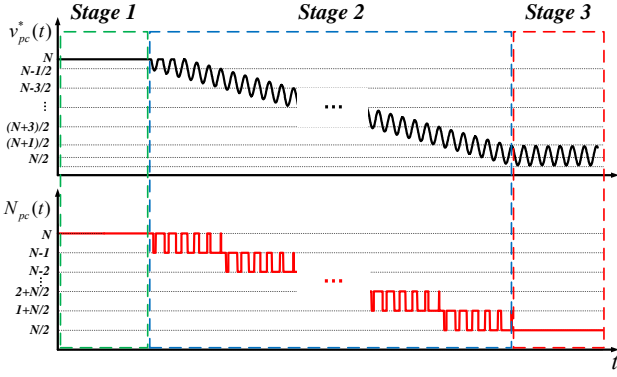


Fig. 8. Pre-charging reference and the number of inserted SMs.

$$\begin{aligned} v_{pc}^*(t) &= v_{ramp}^*(t) + v_{cos}^*(t) \\ &= N - \alpha t + \beta \cos(2\pi ft) \end{aligned} \quad (13)$$

$$N_{pc}(t) = \text{round}(v_{pc}^*(t)) \quad (14)$$

The number of inserted SMs $N_{pc}(t)$ is generated through a round function of $v_{pc}^*(t)$, which is expressed in Equ. (14). $N_{pc}(t)$ is used as the same input as in the upper and lower arm switching algorithm. $N_u(t)$ and $N_l(t)$ used in the afore-mentioned general NLC modulation are the same as $N_{pc}(t)$.

Fig. 8 shows a graph of $v_{pc}^*(t)$ and $N_{pc}(t)$ over time and the operating status accordingly. $v_{pc}^*(t)$ and $N_{pc}(t)$ prior to pre-charging are constant as N . $v_{pc}^*(t)$ and $N_{pc}(t)$ during pre-charging are expressed in Eqs. (13)-(14). $v_{pc}^*(t)$ is decreased according to the gradient constant α from N , and then it repeats on and off by a single SM in every range by the cosine function. The switching frequency for each SM is the same as the frequency of $v_{cos}^*(t)$. The larger the α results in a faster charging speed. $N_{pc}(t)$ is decreased by one over time, which indicates that the number of bypassed SMs is increased by 1.

After pre-charging is completed, $v_{pc}^*(t)$ produces a voltage of $N/2 + \beta \cos(2\pi ft)$. Since the MMC consisting of N SMs per arm has to maintain the number of inserted SMs per leg at N during normal operation, the output of $N_{pc}(t)$ can be different according to N . If N is an odd number, $N_{pc}(t)$ vibrates at a duty ratio of 0.5 between $(N-1)/2$ and $(N+1)/2$ thereby maintaining the average number of inserted SMs per leg to N .

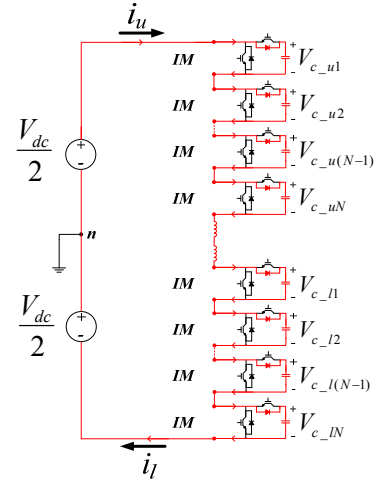
However, if N is an even number, $N_{pc}(t)$ produces $N/2$. Here, the range of $v_{pc}^*(t)$, in which $N_{pc}(t)$ has to be produced as $N/2$, is shown in Equ. (15).

$$\frac{N-1}{2} < \frac{N}{2} + \beta \cos(2\pi ft) < \frac{N+1}{2} \quad (15)$$

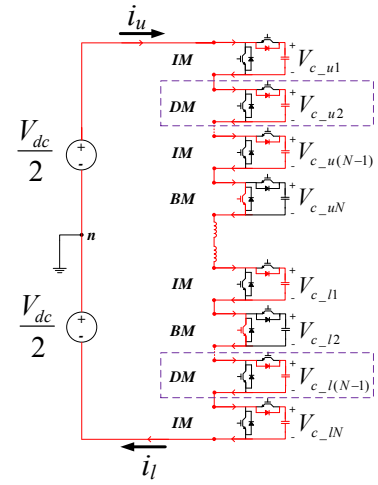
The range of β that can satisfy (15) is shown in (16).

$$0 < \beta < \frac{1}{2} \quad (16)$$

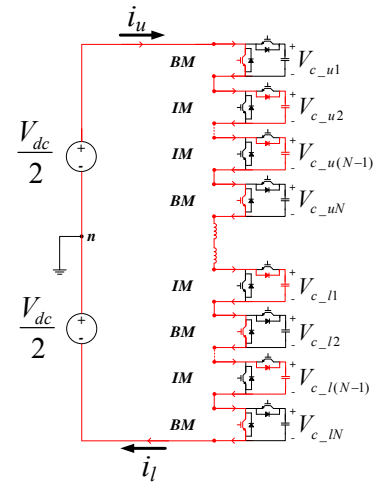
Fig. 9 shows the SM operation of a single-phase MMC according to the operating range. When the DC voltage V_{dc} is applied to series connected SMs, i_u and i_l , which are the



(a) Prior to pre-charging.



(b) During pre-charging.



(c) After pre-charging.

Fig. 9. MMC SM operation according to operating region.

currents flowing through the upper and lower arms, are the same as the current flowing from the DC source. The SM capacitor voltage builds up to $V_{c_{-ux}}$ and $V_{c_{-lx}}$ (Note that $x = 1, 2, \dots, N$).

TABLE I

SM OPERATION MODE

ACCORDING TO SWITCHING STATE AND CURRENT DIRECTION

	$i_{SM} > 0$	$i_{SM} < 0$
Insert mode		
Bypass mode		

Fig. 9(a) shows the operation prior to pre-charging, in which the switching operation of the MMC SM does not occur. All of the SM capacitor voltages are charged equally at $V_{dc} / 2N$. Since the voltage sum for all of the SM capacitors is the same as V_{dc} , the arm current does not flow.

Fig. 9(b) shows the pre-charging operation, in which the SM of the MMC performs the switching operation selectively according to the reference. Here, the operation status of the SMs is classified into the insert mode (IM), the bypass mode (BM), and the duty mode (DM). The IM and BM, depending on the direction of the current i_{SM} flowing in the SM, are summarized in Table I. In the IM, S_1 and S_2 are on and off, respectively. It shows a status where the SM capacitors can be charged or discharged according to the direction of i_{SM} . On the other hand, in the BM, S_1 and S_2 are off and on, respectively. This shows a status where the current does not flow through the SM capacitors due to bypassing. In the DM, changes from the IM to the BM are iterated during the switching period T_s according to the reference. When the SMs in the DM are bypassed, the arm current is increased to charge the capacitors in the other SMs operated with the IM. On the other hand, the arm current is decreased when the SMs in the DM are inserted. The SM operated in the DM is determined by the voltage balancing algorithm during every T_s to make the voltage in the SM capacitors of each arm constant. Whenever $v_{ramp}^*(t)$ is decreased by 1, the number of SMs in the BM is increased by 1. Meanwhile, the number of SMs in the IM is decreased by 1. The number of SMs in the DM is always one, and the number of SMs for each mode is summarized in Table 2 according to the range of $v_{ramp}^*(t)$. When $v_{ramp}^*(t)$ becomes $N/2$, the pre-charging is completed and $v_{ramp}^*(t)$ is maintained at $N/2$.

Fig. 9(c) shows the standby state until the additional MMC operation is started after the pre-charging is complete. Each of the SM capacitor voltages is charged equally at V_{dc} / N . Since no more charging occurs in the standby state, the arm

TABLE II

NUMBER OF SM FOR OPERATION MODE

ACCORDING TO A RANGE OF FIRST-ORDER FUNCTION REFERENCE

Range of function	Operation Mode	BM	IM	DM
$N - 1 < v_{ramp}^*(t) \leq N$		0	$N - 1$	1
$N - 2 < v_{ramp}^*(t) \leq N - 1$		1	$N - 2$	1
\vdots		\vdots	\vdots	\vdots
$\frac{N}{2} + 1 < v_{ramp}^*(t) \leq \frac{N}{2} + 2$		$\frac{N}{2} - 2$	$\frac{N}{2} + 1$	1
$\frac{N}{2} < v_{ramp}^*(t) \leq \frac{N}{2} + 1$		$\frac{N}{2} - 1$	$\frac{N}{2}$	1

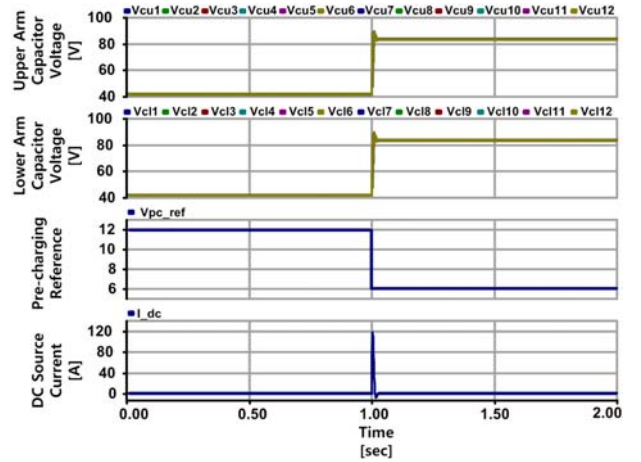


Fig. 10. Simulation results during initial startup of MMC without pre-charging method.

current does not flow. If N is an even number, $N_{pc}(t)$ produces $N/2$. On the other hand, if N is an odd number, $N_{pc}(t)$ vibrates between $(N-1)/2$ and $(N+1)/2$ with a duty ratio of 0.5. Accordingly, a single SM is operated under the DM with 0.5 of a duty ratio even after the pre-charging is completed.

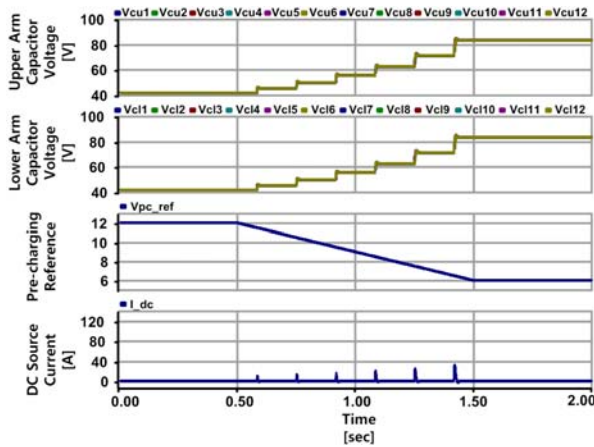
V. COMPUTER SIMULATIONS

The power circuit of the 3-phase 10kVA MMC used in the computer simulations consists of 12 SMs per arm which has an identical configuration shown in Fig. 1. Table 3 summarizes the circuit parameters used in the simulations.

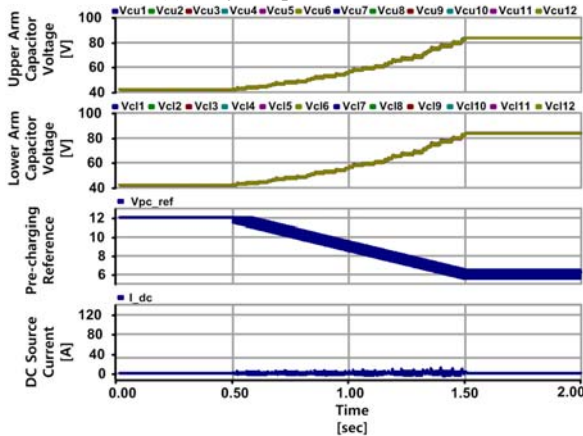
Fig. 10 shows simulation results during the initial startup of the MMC without pre-charging, in which the initial startup of the MMC is started at 3 sec. The first and second waveforms refer to the voltages of the SM capacitor in the upper and lower arms, and the third waveform refers to the reference. The fourth waveform refers to the current flowing in the MMC. When the reference is changed from 12 to 6 during the initial startup, 6 out of 12 SMs inserted to each

TABLE III
3-PHASE 10kVA MMC PARAMETERS

Parameters	Values
Number of SMs per arm	N 12
Rated Power	S_{rated} 10.0 kVA
DC Voltage	V_{dc} 1.0 kV
SM Capacitor	C_{SM} 3200.0 uF
SM Capacitor ESR	R_{SM} 0.06 Ω
Arm Reactor Inductance	L_{arm} 10.0 mH
Arm Reactor Parasitic Resistance	R_{arm} 0.8 Ω
Filter Reactor Inductance	L_F 6.0 mH
Filter Reactor Parasitic Resistance	R_F 0.5 Ω



(a) Only ramp reference function.



(b) Proposed reference function.

Fig. 11. Simulation results applying pre-charging method.

arm prior to the startup are operated with the BM, decreasing the number of SMs in the IM to six. Accordingly, each capacitor voltage is instantaneously charged from 41.67V to 83.33V and the transient current is increased to 115.6A during the charging process. If current flows inside the MMC, the excessive current stress is applied to the elements, which are likely to be damaged.

Fig. 11 shows simulation results to which proposed pre-charging method was applied. The pre-charging was applied for one sec from 2.5 sec. to 3.5 sec. The first and second waveforms refer to the voltages of the SM capacitors in the upper and lower arms, the third waveform refers to the reference, and the fourth waveform refers to the current flowing into the MMC as the same as in Fig. 8.

Fig. 11(a) shows simulation results to which only the ramp reference function $v_{ramp}^*(t)$ is applied during pre-charging. The reference is maintained at 12 during the pre-charging, which was decreased from 12 to 6 at a gradient of 6 during the pre-charging. Since the size of the reference is decreased from 11.5 by one, the number of SMs per arm at the IM was decreased by one, while the number of SMs in the BM was increased by one. Accordingly, the SM capacitor voltage was charged through six steps in total from 41.67V to 83.33V. Once the charging was completed, the reference was maintained at 6. Whenever the voltage is charged, transient currents are generated so a total of six times of transient currents are generated and the maximum transient current is 29.7A. The magnitude is decreased by 0.257 times without pre-charging. However, it is still sufficient to become a cause of system failure.

Fig. 11(b) shows simulation results to which the proposed reference function is applied during pre-charging. The reference is maintained at 12, which was the same as 9(b) prior to the pre-charging. However, it is decreased since it vibrates via a cosine function and a first-order function during pre-charging. Here, the value of α is set to 6, the frequency of the cosine function is 500Hz and the value of β is set to 0.495. Accordingly, the SM capacitor voltage is gradually charged from 41.67V to 83.33V and the charged current vibrates due to cyclical switching to gradually charge voltage. Here, the mean current is 5A and the maximum transient current is 9.86A. The maximum transient current is decreased by 0.087 times compared with the results without applying the pre-charging method, and 0.337 times compared with the results obtained by only applying $v_{ramp}^*(t)$.

VI. HARDWARE EXPERIMENTS

Fig. 12 shows a hardware prototype for the 13-level 3-phase MMC with 10 kVA rating, which was manufactured in the lab based on the computer simulations. The circuit parameters are same as those summarized in Table 3. It consisted of 72 SMs which have 24 SMs per phase. The control system consists of one master controller, which is a host controller, and 6 arm controllers which are slave controllers. The master controller controls the overall system operation, such as the power control and the voltage control. The arm controllers control each of the arms such as the voltage balancing for the SM capacitor and the switching pulse generation.

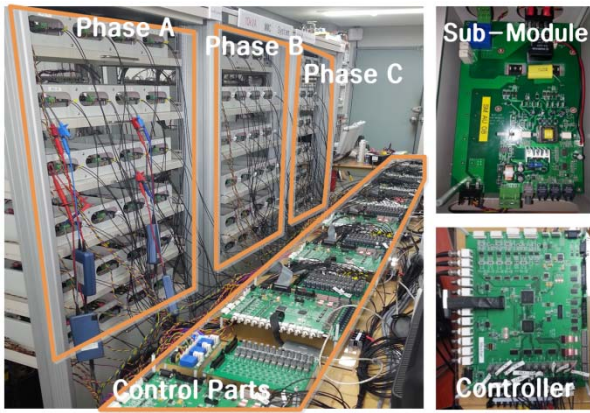
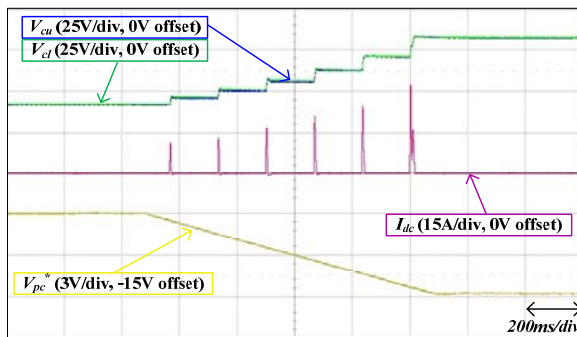
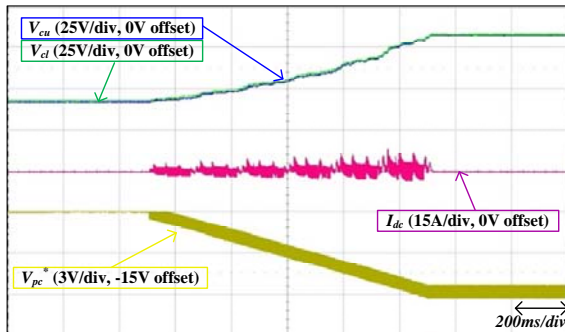


Fig. 12. Hardware prototype for 13-level 3-phase MMC with 10 kVA rating.



(a) Only ramp reference function.



(b) Proposed reference function.

Fig. 13. Experimental results applying pre-charging method.

Fig. 13 shows experimental results of the pre-charging to which the ramp function reference and the proposed reference were applied. Blue and green colors refer to the SM voltages of the upper and lower arms, red color refers to the arm current, and yellow color refers to the reference. The charging time was set to 1 sec., which is the same as in the simulation.

Fig. 13(a) shows experimental results when the ramp reference function was applied. Since the reference is decreased at a constant value, the SM capacitors in the upper and lower arms are charged over six steps. Whenever the SM capacitor voltages are increased, the transient charging currents are generated. Since the SM capacitor voltages to be

charged become higher, the transient charging current is increased and the maximum transient current is about 32.30A.

Fig. 13(b) shows experimental results when the proposed method was applied. The reference is maintained at 12 prior to charging and the reference is decreased while vibrating by a cosine function during charging so that the SM capacitors are gradually charged. Once charging is complete, the reference is maintained at $6 + 0.495\cos(2\pi \cdot 500t)$. The transient charging current is vibrated due to cyclical switching. As the SM capacitor voltages become higher, the transient charging current is increased. Here, the maximum transient current is approximately 8.28A, which was decreased by 0.256 times compared to the one that applied the ramp reference function.

VII. CONCLUSIONS

In this paper, an improved pre-charging method for MMC operated in the NLC modulation was proposed. The proposed pre-charging method employs a cosine function and a ramp function as references to obtain the PWM effect without a carrier.

In order to verify the superiority of the proposed method, computer simulations for a 3-phase 13-level MMC with a 10kVA rating were conducted by applying the ramp reference function and the proposed reference function. Based on the obtained simulation results, a hardware prototype was manufactured in the lab for experimental verification.

The simulation and experimental results confirm that the transient charging current during the initial startup of the MMC can be greatly reduced for safe operation. The proposed method does not incur an additional cost because an additional pre-charging circuit is not required. Therefore, the system stability and reliability can be improved by applying the proposed method because it can protect various elements such as the switches, resistances, and capacitors used in systems.

ACKNOWLEDGMENT

This work was supported by the National Research Foundation (NRF) grant funded by the Korea Ministry of Science, ICT and Future Planning (NRF-2015R1A2A2A01004102)

REFERENCES

- [1] G. Bergna, E. Berne, P. Egrot, P. Lefranc, A. Arzande, J.-C. Vannier, and M. Molinas, "An energy-based controller for HVDC modular multilevel converter in decoupled double synchronous reference frame for voltage oscillation reduction," *IEEE Trans. Ind. Electron.*, Vol. 60, No. 6, pp. 2360-2371, Jun. 2013.
- [2] E. Solas, G. Abad, J. A. Barrena, S. Aurtenetxea, A. Cárcar, and L. Zając, "Modular multilevel converter with different

- submodule concepts — Part II: experimental validation and comparison for HVDC application,” *IEEE Trans. Ind. Electron.*, Vol. 60, No. 10, pp. 4536-4545, Oct. 2013.
- [3] S. Rohner, S. Bernet, M. Hiller, and R. Sommer, “Modulation, losses, and semiconductor requirements of modular multilevel converters,” *IEEE Trans. Ind. Electron.*, Vol. 57, No. 8, pp. 2633-2642, Aug. 2010.
- [4] M. Saeedifard and R. Iravani, “Dynamic performance of a modular multilevel back-to-back HVDC system,” *IEEE Trans. Power Del.*, Vol. 25, No. 4, pp. 2903-2912, Oct. 2010.
- [5] M. Glinka, “Prototype of multiphase modular-multilevel-converter with 2 MW power rating and 17-level-output-voltage,” in *IEEE 35th Annual Power Electronics Specialists Conference (PESC)*, pp. 2572-2576, Jun. 2004.
- [6] M. Hagiwara and H. Akagi, “PWM control and experiment of modular multilevel converters,” in *IEEE Power Electronics Specialists Conference*, pp. 154-161, Jun. 2008.
- [7] A. Lesnicar and R. Marquardt, “An innovative modular multilevel converter topology suitable for a wide power range,” in *IEEE Bologna Power Tech Conference Proceedings*, Jun. 2003.
- [8] S. Allebrod, R. Hamerski, and R. Marquardt, “New transformerless, scalable modular multilevel converters for HVDC-transmission,” in *IEEE Power Electronics Specialists Conference (PESC)*, pp. 174-179, Jun. 2008.
- [9] A. Antonopoulos, L. Angquist, and H.-P. Nee, “On dynamics and voltage control of the modular multilevel converter,” in *13th European Conference on Power Electronics and Applications (EPE)*, pp. 1-10, Sep. 2009.
- [10] K. Ilves, A. Antonopoulos, S. Norrga, and H.-P. Nee, “A new modulation method for the modular multilevel converter allowing fundamental switching frequency,” *IEEE Trans. Power Electron.*, Vol. 27, No. 8, pp. 3482-3494, Aug. 2012.
- [11] Q. Tu, Z. Xu, and L. Xu, “Reduced switching-frequency modulation and circulating current suppression for modular multilevel converters,” *IEEE Trans. Power Del.*, Vol. 26, No. 3, pp. 2009-2017, Jul. 2011.
- [12] H. Saad, X. Guillaud, J. Mahseredjian, S. Denetiere, and S. Nguéfeu, “MMC capacitor voltage decoupling and balancing controls,” *IEEE Trans. Power Del.*, Vol. 30, No. 2, pp. 704-712, Apr. 2015.
- [13] Z. Wang, A. Zhang, H. Zhang, C. Zhang, and Y. Bai, “Control strategy for modular multilevel converters in sub-module fault state,” in *IEEE 10th Conference on Industrial Electronics and Applications (ICIEA)*, pp. 369-374, Jun. 2015.
- [14] R. Marquardt and A. Lesnicar, “New concept for high voltage-modular multilevel converter,” in *Proceedings of IEEE PESC*, pp. 1-5, 2004.
- [15] A. Lesnicar and R. Marquardt, “An innovative modular multilevel converter topology suitable for a wide power range,” in *IEEE Bologna Power Tech Conference Proceedings*, pp. 1-6, Jun. 2003.
- [16] J. Xu, C. Zhao, B. Zhang, and L. Lu, “New precharge and submodule capacitor voltage balancing topologies of modular multilevel converter for VSC-HVDC application,” in *Asia-Pacific Power and Energy Engineering Conference (APPEEC)*, pp. 1-4, Mar. 2011.
- [17] A. Das, H. Nademi, and L. Norum, “A method for charging and discharging capacitors in modular multilevel converter,” in *37th Annual Conference on IEEE Industrial Electronics Society (IECON)*, pp. 1058-1062, Nov. 2011.
- [18] K. Shi, F. Shen, D. Lv, P. Lin, M. Chen, and D. Xu, “A novel start-up scheme for modular multilevel converter,” in *IEEE Energy Conversion Congress and Exposition (ECCE)*, pp. 4180-4187, Sep. 2012.
- [19] X. Shi, B. Liu, Z. Wang, Y. Li, L. M. Tolbert, and F. Wang, “Modelling, control design, and analysis of a startup scheme for modular multilevel converters,” *IEEE Trans. Ind. Electron.*, Vol. 62, No. 11, pp. 7009-7024, Nov. 2015.
- [20] P. Hu and D. Jiang, “A level-increased nearest level modulation method for modular multilevel converters,” *IEEE Trans. Power Electron.*, Vol. 30, No. 4, pp. 1836-1842, Apr. 2015.



Kyo-Min Kim was born in Seoul, Korea. He received his B.S. degree in Electrical Engineering from Myongji University. He is currently pursuing his Master's degree at Myongji University. His current research interests include FACTS and MMC for HVDC.



Jae-Hyuk Kim was born in Incheon, Korea. He received his B.S. degree in Electrical Engineering from Myongji University. He is currently pursuing his Ph.D. degree at Myongji University. His current research interests include Semiconductor transformer, FACTS and MMC for HVDC.



Do-Hyun Kim was born in Ulsan, Korea. He received his B.S. degree in Electrical Engineering from Myongji University. He is currently pursuing his Ph.D. degree at Myongji University. His current research interests include Semiconductor transformer, FACTS and MMC for HVDC.



Byung-Moon Han was born in Seoul, Korea. He received his B.S. degree in Electrical Engineering from Seoul National University, Seoul, Korea, in 1976, and his M.S. and Ph.D. degrees from Arizona State University, USA, in 1988 and 1992, respectively. He was with the Westinghouse Electric Corporation as a Senior Research Engineer in the Science and Technology Center, Pittsburg, PA, USA. He is currently a Professor in the Department of Electrical Engineering, Myongji University, Seoul, Korea. His current research interests include power electronics applications for FACTS, custom power, distributed generation, and microgrid.



Jun-Young Lee received his B.S. degree in Electrical Engineering from Korea University, Seoul, in 1993 and his M.S. and Ph.D. degrees in Electrical Engineering from Korea Advanced Institute of Science and Technology(KAIST), Taejon, Korea, in 1996 and 2001, respectively. From 2001 to 2005, he worked as a Manager in Plasma Display Panel Development Group, Samsung SDI where he was involved in circuit and product development. From 2005 to 2008, he worked as a faculty member in the School of Electronics and Computer Engineering, Dankook University. In 2008, he joined the School of Electrical Engineering, Myongji University, as an associate professor. His research interests are in the areas of power electronics which include Converter topology design, soft switching techniques, display driving system, and battery charger system.